

## Inventory of Supplemental Information

### Figures

Many of these figures are described in our covering letter and response to referees. Many of them were generated in response to direct comments from our referees.

Figure S1: FRAP of GFP- $\Delta$ C in metaphase and anaphase and determination of the diffusion constant for cytoplasmic GFP-MHC. This figure shows the controls that the referees requested for our determination of myosin diffusion.

Figure S2: Quantitation of myosin distribution at the equator and poles before and after anaphase onset. This figure shows the change in myosin distribution as cells progress from metaphase to anaphase and was requested to bolster the quantitative rigor of figure 3.

Figure S3: Quantitation of Rho depletion and Kymograph analysis of myosin particle movement. This figure presents both control data (showing the levels of Rho depletion), and contains a kymograph which illustrates the directed flowing of myosin particles towards the cell interior during anaphase.

Figure S4: Cortical flow is not evident in untreated S2 cells. This figure was initially our first figure, but we moved it to the Supplemental materials. It contains kymograph and

FRAP data that shows that cortical flow of myosin is not evident in *Drosophila* S2 cells, and contains the improved controls for FRAP specificity that the referees requested.

## **Movies**

Movie S1 shows the localization of two of the truncated MHC constructs from metaphase to anaphase, is directly related to what is shown in Figure 1, and was requested by our referees. Movies S2, S3, and S4 all show the TIRF localization of myosin from metaphase to anaphase and are made from the cells shown in Figure 3.

Movie S1: GFP- $\Delta$ Motor-MHC is able to target to the equatorial cortex while GFP- $\Delta$ N-MHC forms structures in anaphase but cannot be targeted to the cytokinetic furrow.

Movie S2: TIRF localization of wild type RLC-GFP and RLC[E20E21]-GFP from metaphase to anaphase.

Movie S3: TIRF localization of wild-type RLC-GFP in Rho-depleted cells.

Movie S4: TIRF localization of a RLC[E20E21]-GFP in cells depleted of Rho.

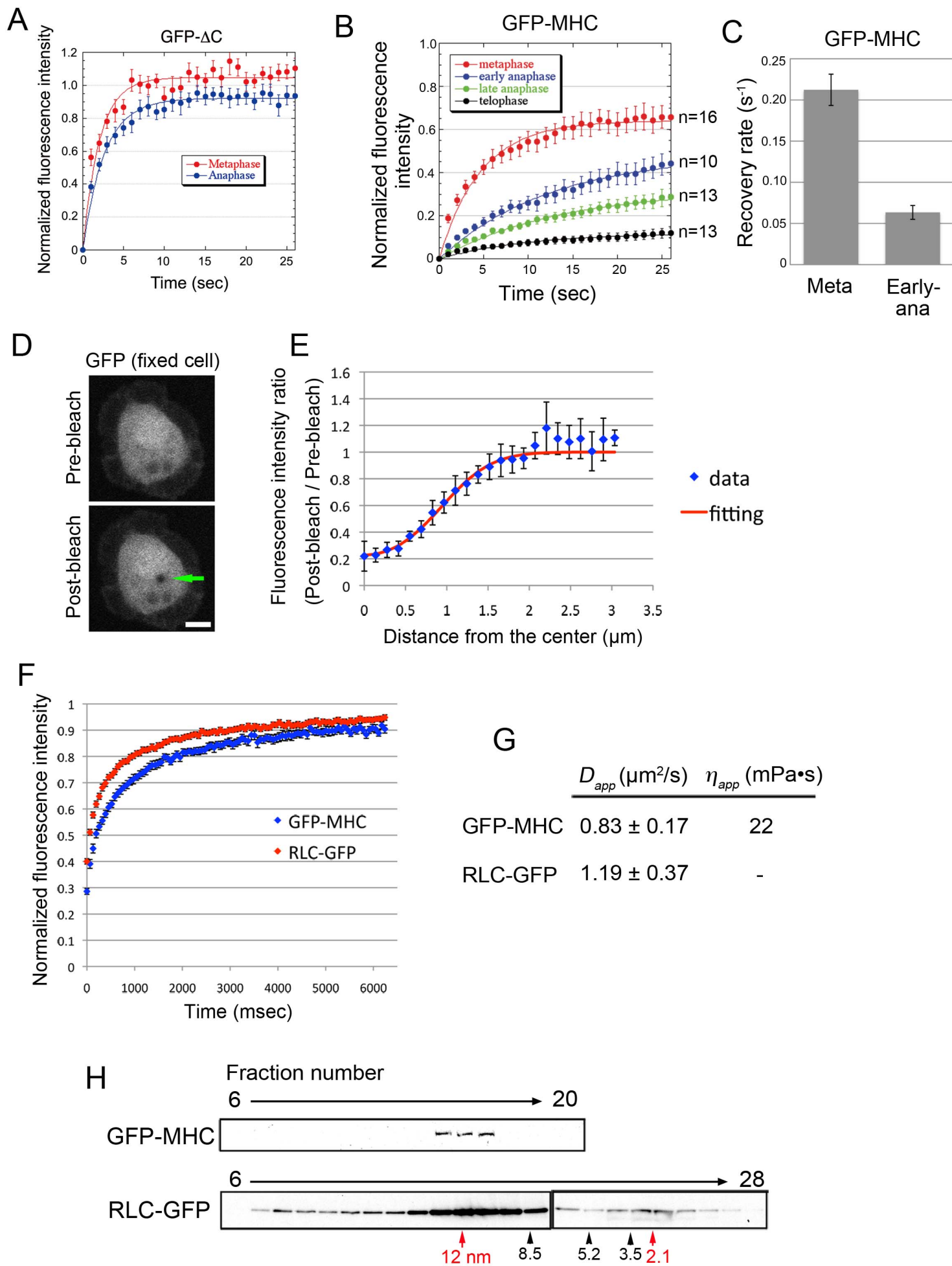


Figure S2

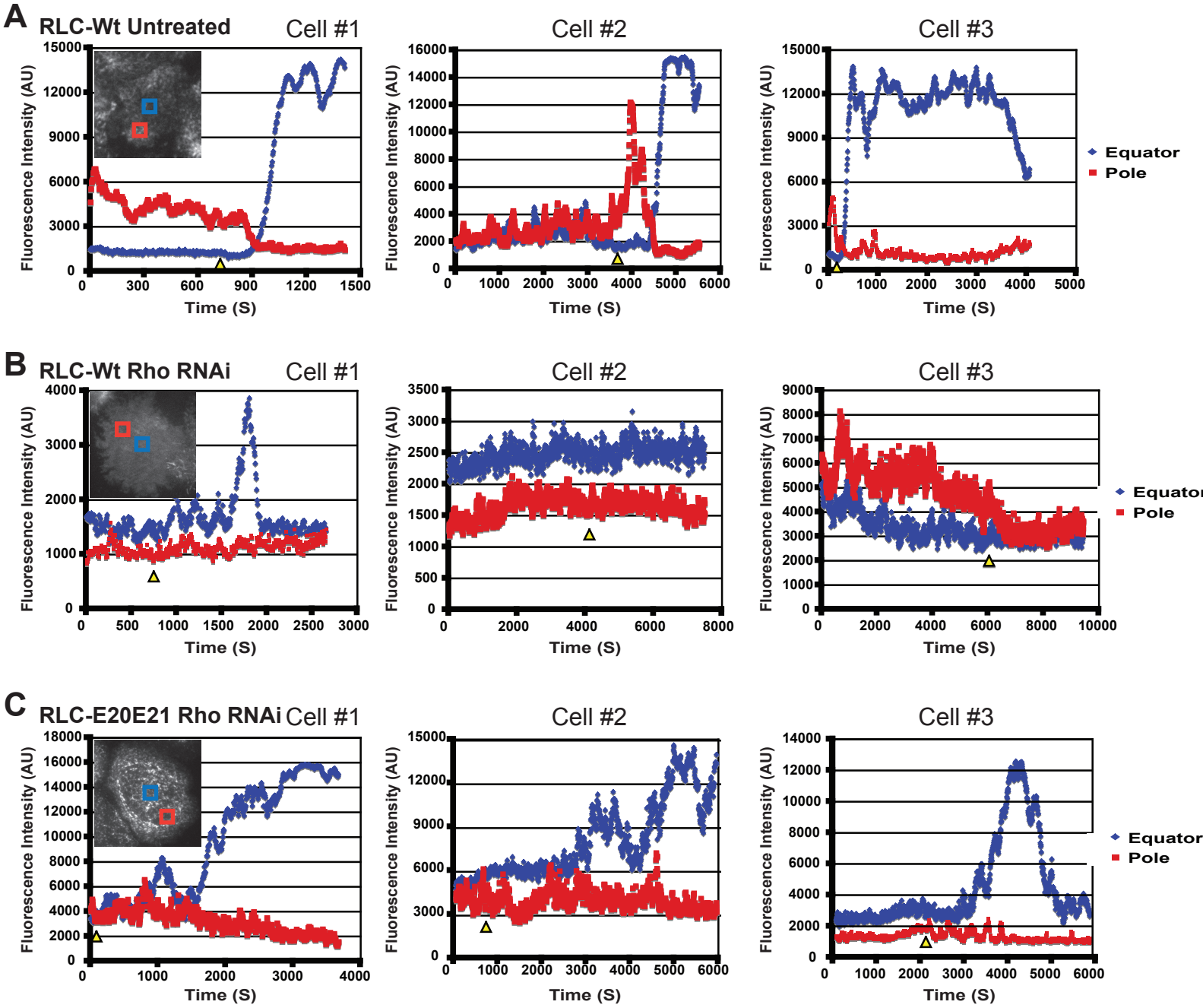
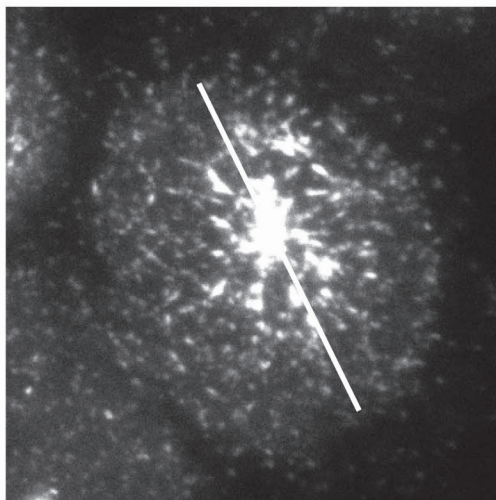
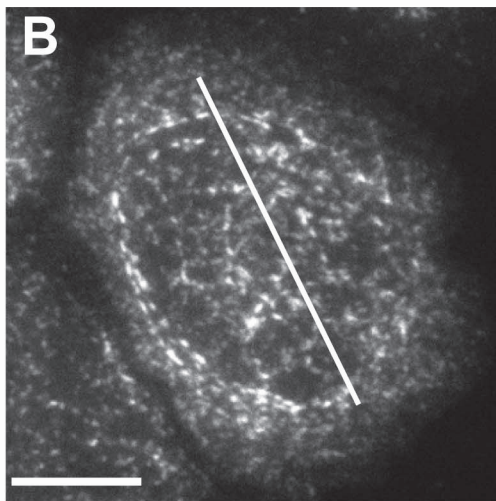
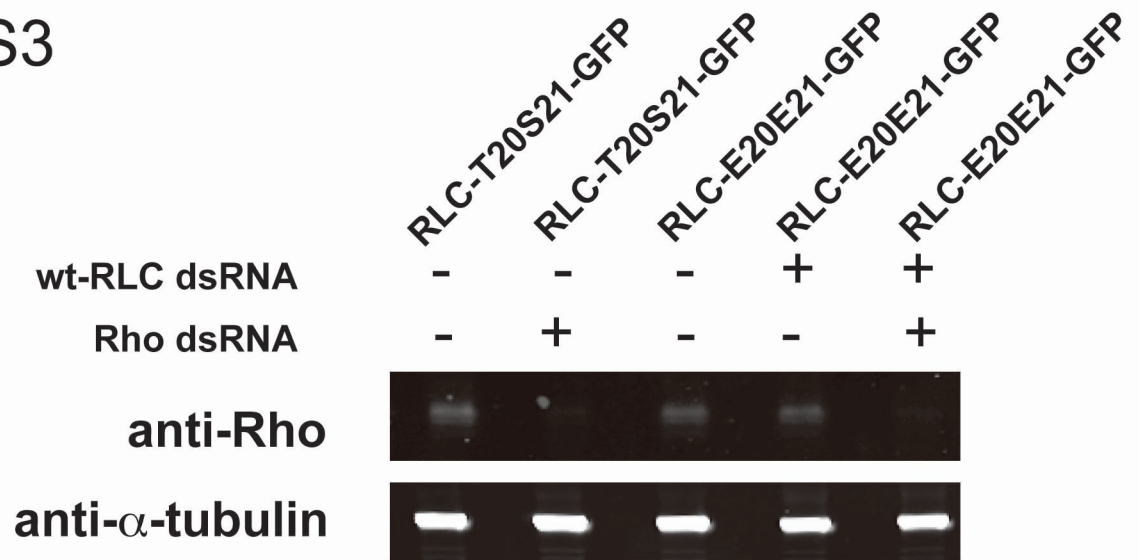


Figure S3

A



41:50

B'

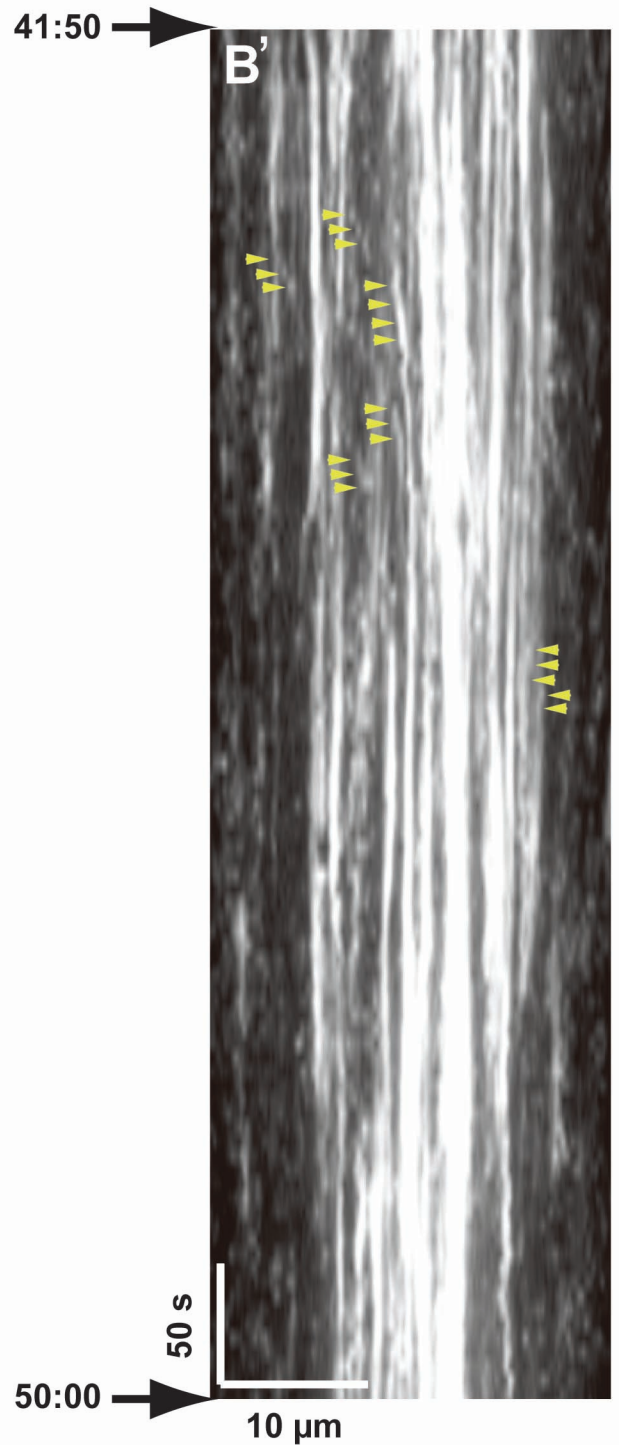
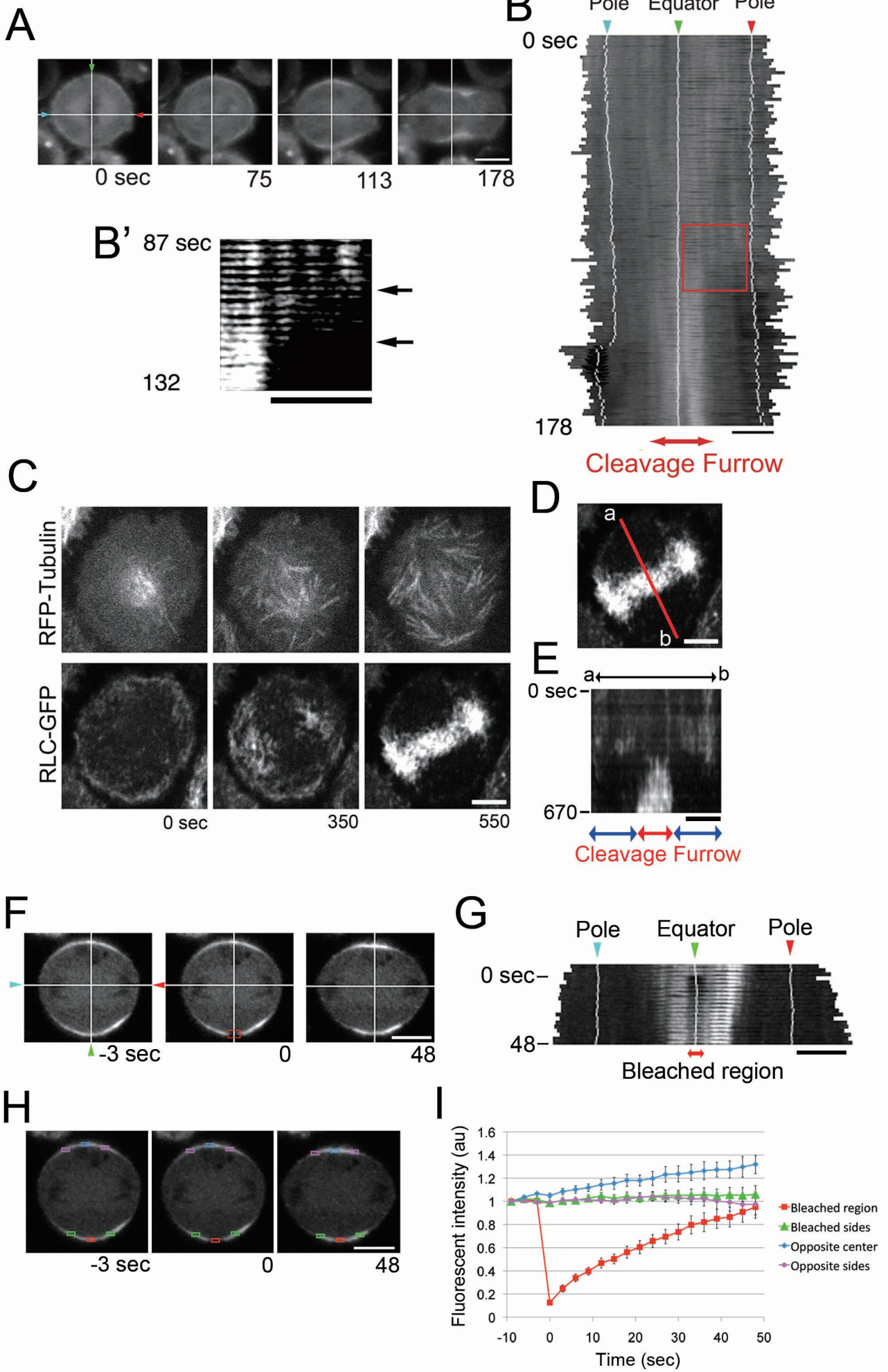


Figure S4



## Supplemental Figure Legends

Figure S1: FRAP of GFP- $\Delta$ C in metaphase and anaphase and determination of the diffusion constant for cytoplasmic GFP-MHC.

The recovery rates of  $\Delta$ C MHC construct both in metaphase ( $0.55 \pm 0.11 \text{ s}^{-1}$ , n=8) and anaphase ( $0.34 \pm 0.03 \text{ s}^{-1}$ , n= 11) were much larger than those of the full-length MHC construct (see Figure S2). (B) FRAP of GFP-MHC during cell division. Anaphase/telophase was divided into three phases as described in figure 2A. Error bars represent SEM. Observed cell number is indicated for each sample. (C) Mean recovery rate of GFP-MHC in metaphase and early anaphase, with SEM. (D) S2 cells expressing GFP were fixed and bleached to obtain the photobleach profile. Green arrow indicates the bleached area. Bar, 5 $\mu$ m. (E) Photobleach profile of the Gaussian laser beam used for FRAP of cytoplasmic myosin (n=5;  $\pm$  SD). The equation used for curve fitting is described in supplemental text. (F) FRAP of cytoplasmic GFP-MHC (n=13;  $\pm$  SEM) and RLC-GFP (n=24;  $\pm$  SEM). (G) Gel filtration of S2 cell extract containing GFP-tagged myosin subunits. GFP-MHC was detected in a single peak corresponding to single myosin molecules (which are hexamers of two heavy chains and four light chains) (stokes radius of  $\sim$ 12 nm), while RLC-GFP was detected in the peaks corresponding to single myosin molecules and monomeric RLC-GFP ( $\sim$ 2.1 nm). (H) Diffusion coefficient of cytoplasmic myosin and apparent viscosity of cytoplasm for myosin molecules were determined as described in the supplemental text. Apparent viscosity was determined only for GFP-MHC, since RLC-GFP could exist in the cytoplasm as two subpopulations, one of single myosin molecules and one of RLC-GFP monomers with an unknown ratio between the two populations.

Figure S2: Quantitation of myosin distribution at the equator and poles before and after anaphase onset.

S2 cells expressing wild-type RLC-GFP or RLC-E20E21-GFP and mCh-Tubulin were treated with the indicated dsRNAs, flattened on ConA and imaged in TIRF from metaphase through anaphase. We measured the average fluorescence in a 3  $\mu\text{m}$  square area of the cell cortex either at the equator or pole from metaphase through anaphase and then plotted the average fluorescence in these areas over time.

Figure S3: Quantitation of Rho depletion and Kymograph analysis of myosin particle movement.

S2 cells expressing wild-type RLC-GFP or RLC-E20E21-GFP and mCh-Tubulin were treated with the indicated dsRNAs, lysed in sample buffer and the total cellular proteins were separated by PAGE electrophoresis, blotted to nitrocellulose. The blots were probed with antibodies to RhoA and  $\alpha$ -tubulin. Bands were detected with Alexa-680 labeled anti-mouse secondaries and observed with a Licor Odyssey. We clearly observe equivalent Rho depletion efficiency in both cell lines.

The S2 cell shown in Figure 5c expressing the phosphomimetic RLC and mCh-tubulin and treated with dsRNAs to deplete the endogenous RLC and RhoA was imaged in TIRF. The line shown in (B) was used to generate a kymograph from metaphase through late anaphase. The lateral movement of particles can be seen as diagonal lines in the kymograph (B'; arrowheads) which is a subsection of the total kymograph and covers the time frame indicated. Bar, 10  $\mu\text{m}$ .

Figure S4: Cortical flow is not evident in untreated S2 cells.

(A) RLC-GFP was observed in unflattened cells. Equatorial accumulation and polar exclusion were detected after anaphase (113 – 178 sec). (B) A kymograph was generated along the cortex indicated with arrowheads in (A). (B') The region indicated by the red box in (B) was magnified. GFP signals initially observed near the pole disappeared in anaphase without showing inward movement (arrow). (C) RLC-GFP and RFP-tubulin were observed in cells flattened on concanavalin-A (Con-A) -coated dishes. Images of the bottom surface of the cells were acquired every 5 seconds (n=7). The Con-A-dependent flattening of cells minimizes the probability that GFP movement from a different focal plane is missed. (D, E) By generating kymographs along the pole-to-pole axis (red line, top), we confirmed equatorial accumulation of RLC-GFP during anaphase (red arrow zone) and exclusion from the pole under this condition (blue arrow zone). However, we could not detect any inward movement of GFP signals along the cortex, suggesting that cortical flow may not be prevalent in S2 cells. (F) To look more carefully for cortical flow of myosin filaments, we photobleached the RLC-GFP at the equatorial cortex in unflattened cells in early anaphase and then monitored the recovery of the GFP signal (n= 7). The red box indicates the bleached region. (G) A kymograph was generated along the cortex that contains the photobleached area. Fluorescence recovered gradually along the bleached area, but we could not detect lateral movement of unbleached GFP signals into the bleached area. (H) Fluorescence intensities in the bleached region (red boxes), regions flanking the bleached area (bleached sides; green boxes), the equatorial region of the cortex on the opposite side of the cell (opposite center; blue boxes) and regions flanking the opposite center (opposite sides; purple

boxes) were monitored during FRAP. (I) A quantification of fluctuation of the fluorescence intensity ( $\pm$  SEM) in each region depicted in D (n=7). Photobleaching in the equatorial cortex did not affect fluorescence intensity in the flanking cortical regions, suggesting that lateral movement of myosin is absent along the cortex. Bars 5  $\mu$ m.

### **Supplemental Movies:**

Movie S1: GFP- $\Delta$ Motor-MHC is able to target to the equatorial cortex while GFP- $\Delta$ N-MHC forms structures in anaphase but cannot be targeted to the cytokinetic furrow.

Upper Cell: An S2 cell expressing GFP- $\Delta$ Motor-MHC and mCh-tubulin was treated with a dsRNA that targets the motor domain of the endogenous MHC, plated on conA coated coverslip, and imaged from metaphase to anaphase. Movie is shown at 400x real time. Field of view is 25  $\mu$ m x 25  $\mu$ m.

Lower Cell: An S2 cell expressing GFP- $\Delta$ N-MHC was treated with a dsRNA that targets the motor domain of the endogenous MHC, plated on a conA coated coverslip, and imaged with a spinning disc confocal from metaphase to anaphase. Movie is shown at 400x real time. Field of view is 33  $\mu$ m x 25  $\mu$ m.

Movie S2: TIRF localization of wild type RLC-GFP and RLC[E20E21]-GFP from metaphase to anaphase.

Upper Cell: An S2 cell expressing RLC-GFP and mCh-tubulin was plated on conA and imaged in TIRF from metaphase to anaphase. Movie is shown at 100x real time. Field of view is 27.5  $\mu$ m x 27.5  $\mu$ m.

Lower Cell: An S2 cell expressing RLC[E20E21]-GFP and mCh-tubulin was treated with a dsRNA to deplete the endogenous RLC, plated on conA and imaged from metaphase to anaphase. A large accumulation of myosin at the cortex is evident in many cells, and it becomes incorporated into the nascent cytokinetic ring. Movie is shown at 250x real time. Field of view is 23  $\mu\text{m}$  x 23  $\mu\text{m}$ .

Movie S3: TIRF localization of wild-type RLC-GFP in Rho-depleted cells

Upper Cell: An S2 cell expressing RLC-GFP and mCh-tubulin was treated with a dsRNA that targets Rho, plated on conA and imaged in TIRF from metaphase to anaphase. The lack of any myosin assembly in the TIRF field indicates that Rho has been efficiently depleted. The majority of Rho-depleted cells showed a similar distribution of myosin. Movie is shown at 250x real time. Field of view is 25  $\mu\text{m}$  x 25  $\mu\text{m}$ .

Lower Cell: In some of the cells treated as described above highly dynamic flares of myosin assembly can be seen locally, indicative of low levels of residual Rho, a phenomenon seen in approximately 20% of cells. Movie is shown at 250x real time. Field of view is 41  $\mu\text{m}$  x 41  $\mu\text{m}$

Movie S4: TIRF localization of a RLC[E20E21]-GFP in cells depleted of Rho.

An S2 cell expressing RLC[E20E21]-GFP was treated with dsRNAs that target the endogenous RLC and Rho, plated on conA and imaged in TIRF from metaphase. The myosin appears to be much more loosely organized and transiently localized compared to cells where Rho is present, and particles of myosin can be seen moving laterally along the cortex. Movie is shown at 250x real time. Field of view is 39  $\mu\text{m}$  x 39  $\mu\text{m}$ .

## Experimental Procedures

### Cell lines, plasmids, and RNA interference

Drosophila S2 cells were cultured in Schneider's insect cell media (Sigma or Invitrogen) supplemented with 10% FCS at 22° C. Cells expressing RLC-GFP and RFP- $\alpha$ -tubulin are described in [1]. The plasmid for GFP-myosin II heavy chain expression (pUbp-GFP-Zipper) was a kind gift of Dr. Dan Kiehart (Duke University) and the pMT-GFP-Zipper 1350-1940 (aa1350-1940) construct was a gift of Dr. Kenneth Prehoda (University of Oregon). GFP- $\Delta$ N (aa 1111-2011) and GFP- $\Delta$ Motor (aa 809-2011) were created by PCR and ligated into the pMT-GFP-W Gateway Expression vector [2]. GFP- $\Delta$ C (aa1-1903) was created by SalI digestion of the pUbp-GFP-Zipper plasmid. This resulted in deletion of amino acid residues 1904–2011 of Zipper and addition of 11 amino acid residues (GTAGPGSTGSR) after residue V1903. Transfection was performed using FuGENE HD (Roche, Indianapolis, IN) according to the manufacturer's instruction. RNA interference (RNAi) was performed following [3]. Templates for transcription of dsRNA were generated by PCR using primers: RLC-Endodepletion - 5'-CATCAACTTCACCATGTTCC-3' and 5'-TTACTGCTCATCCTTGTTCC-3', Zipper-motor - 5'-CCTAAAGCCACTGACAAGACG-3' and 5'-CGGTACAAGTTCGAGTCAAGC-3', and Rho- 5' - CGCGAATATATAAAACAGAACGG - 3' and 5' - GCCACATAATTCTCGAATACGG - 3' with the T7 promoter sequence attached to the 5' end of each. dsRNAs was transcribed using in vitro Transcription T7 kit (TaKaRa, Tokyo, Japan), and purified using MEGAclear (Ambion, Austin, TX). For

full depletion of the endogenous Zipper protein, cells were treated twice with dsRNA (once at day 0 and again at day 3-4) and exposed to dsRNA for a seven day period.

#### Live cell imaging and FRAP (fluorescence recovery after photobleaching)

For time-lapse imaging, an FV300 confocal microscope equipped with a plan apo 100X objective lens (Olympus, Tokyo, Japan), a Zeiss Axiovert 200M equipped with a spinning-disk scanhead and laser system (Yokogawa CS10, Yokogawa Electronics, Japan; Solamere, Salt Lake City, Utah), Orca II ERG CCD camera (Hamamatsu Photonics, Japan), and 100x 1.45 n.a. objective (Carl Zeiss, Thornwood, New York) were used. Dual-color TIRF was performed as previously described [4]. To generate kymographs, a region of interest (ROI) was selected along the cortex in each frame of the time-lapse image sequence, linearized using “ROI” plugin of Image J, and stacked in order into a picture with the equator arranged in line.

FRAP experiments for cytoplasmic myosin was performed with FV1000 (Olympus) confocal microscope. Images were acquired every 65 msec. Photobleaching was conducted using a LD 405 nm laser (50mW 30% for 10 msec) after 3 frames of prebleaching imaging. In this condition, we could achieve sufficient depth of photobleaching throughout the specimen (not shown). Apparent 2-dimensional diffusion coefficients[4] of GFP-tagged myosin subunits in cytoplasm were determined as described in Axelrod et al. 1976 with slight modification; To obtain the photobleaching profile of the Gaussian laser beam, GFP-expressing cells were fixed with PFA and photobleached in the identical condition as the FRAP experiment. Pre-

bleach and post-bleach fluorescence intensities were measured along a line across the bleached region, and a photobleaching profile was obtained by dividing the latter by the former (FigureS1D-E). The profile was fitted using the equation;

$$C(r) = \exp[-K \times \{\exp(-2r^2/w^2)\}]$$

where  $C(r)$  is the ratio of post-bleach intensity to the pre-bleach intensity at a distance of  $r$  from the center of the bleached region,  $w$  is radius of a Gaussian beam at  $e^{-2}$  intensity and  $K$  represents bleaching parameter (Axelrod et al. 1976). In our experimental condition,  $w$  was 1.3  $\mu\text{m}$ , and  $K$  was 1.48.

Fluorescence recovery curves obtained by FRAP were fitted using the equation;

$$I(t) = a + b \sum_{n=0}^{40} \left[ \frac{(-K)^n}{n!} \left[ 1 + n \left( 1 + 2t/\tau_D \right) \right]^{-1} \right]$$

where  $a$  and  $b$  is constants, and  $\tau_D$  is diffusion time.

Diffusion coefficient  $D$  was calculated using the equation;

$$D = w^2 / 4\tau_D$$

To estimate molecular size of cytoplasmic myosin, cell extract prepared from S2 cell

expressing GFP-MHC or RLC-GFP were subjected to gel filtration chromatography using TSK G5000PWXL (Tosoh). GFP-tagged myosin subunits were detected by western blotting using anti-GFP (Clontech). Stokes radius of GFP-tagged myosin was calculated according to REF. Apparent viscosity  $\eta$  of cytosol for GFP-MHC was estimated by Einstein relation;

$$\eta = \frac{kT}{6\pi Dr}$$

where  $k$  is Boltzmann's constant,  $T$  is absolute temperature and  $r$  is stokes radius estimated from gel filtration.